



**HAL**  
open science

## On the effective charge of hydrophobic polyelectrolytes

Alexei Chepelianskii, Farshid Mohammad-Rafiee, Elie Raphael

► **To cite this version:**

Alexei Chepelianskii, Farshid Mohammad-Rafiee, Elie Raphael. On the effective charge of hydrophobic polyelectrolytes. 2007. hal-00179022v1

**HAL Id: hal-00179022**

**<https://hal.science/hal-00179022v1>**

Preprint submitted on 12 Oct 2007 (v1), last revised 24 Apr 2008 (v2)

**HAL** is a multi-disciplinary open access archive for the deposit and dissemination of scientific research documents, whether they are published or not. The documents may come from teaching and research institutions in France or abroad, or from public or private research centers.

L'archive ouverte pluridisciplinaire **HAL**, est destinée au dépôt et à la diffusion de documents scientifiques de niveau recherche, publiés ou non, émanant des établissements d'enseignement et de recherche français ou étrangers, des laboratoires publics ou privés.

# On the effective charge of hydrophobic polyelectrolytes

A. Chepelianskii <sup>(a)</sup>, F. Mohammad-Rafiee <sup>(b,c)</sup> and E. Raphaël <sup>(c)</sup>

<sup>(a)</sup> *Laboratoire de Physique des Solides, UMR CNRS 8502,  
Bât. 510, Université Paris-Sud, 91405 Orsay, France*

<sup>(b)</sup> *Institute for Advanced Studies in Basic Sciences (IASBS),  
Zanjan 45195, P.O. Box 45195-1159, Iran. and*

<sup>(c)</sup> *Laboratoire Physico-Chimie Théorique, UMR CNRS Gulliver 7083,  
ESPCI, 10 rue Vauquelin, 75005 Paris, France*

(Dated: October 12, 2007)

In this paper we analyze the behavior of hydrophobic polyelectrolytes. It has been proposed that this system adopts a pearl-necklace structure reminiscent of the Rayleigh instability of a charged droplet. Using a Poisson-Boltzmann approach, we calculate the counterion distribution around a given pearl assuming the latter to be penetrable for the counterions. This allows us to calculate the effective electric charge of the pearl as a function of the chemical charge. Our predictions are in very good agreement with the recent experimental measurements of the effective charge by Essafi *et al.* (Europhys. Lett. **71**, 938 (2005)). Our results allow to understand the large deviation from the Manning law observed in these experiments.

PACS numbers: 82.35.Rs, 83.80.Rs, 61.25.Hq, 82.45.Gj

The study of polyelectrolytes has attracted an increased attention in the scientific community over the last decades. This interest is motivated by technological applications including viscosity modifiers, or leak protectors and by the hope that advances in this domain will allow to unravel the structure of complex biological macromolecules. In these systems, the Coulomb interactions leads to many remarkable and counterintuitive phenomena [1, 2, 3, 4, 5]. A celebrated example is the Manning-Oosawa counterion condensation. In his classical work [1], Manning showed that a charged rodlike polymer can create such a strong attractive force on its counterions, that a finite fraction condenses onto the polymer backbone. This condensation-phenomenon was also described by Oosawa within a two state model [2]. It leads to an effective decrease of the polymer charge, the macroscopic properties of the polyelectrolyte, like migration in an electrophoresis experiment, are not determined by its bare charge, but by an effective charge that accounts for the Manning-Oosawa counterion condensation. It is now well-established that counterion condensation is a fundamental phenomenon, and that it occurs in many important systems including DNA in both its double-stranded and single-stranded form [6]. It was predicted in [1] that condensation occurs whenever the average distance  $l$  between co-ions on the polymer backbone is smaller than the Bjerrum length  $\ell_B = q^2/(4\pi\epsilon\epsilon_0k_B T)$ , where  $q$  is the co-ion charge,  $k_B T$  the thermal energy and  $\epsilon$  the (relative) dielectric constant of the solvent. This condensation is expected to lead to an average charge density of  $q/\ell_B$  on the polymer backbone. Since the original prediction by Manning, important efforts have been devoted to a description of the Manning-Oosawa condensation within the Poisson-Boltzmann theory [7, 8, 9], establishing the influence of salt, the thickness of the condensed counterion layer and the corrections induced by short range

correlation.

While the conformation of many polyelectrolytes is well described by the rod-like model, many proteins organize into complex self-assembled structures [10]. A challenging and very important topic is the extent to which the structural complexity of biological enzymes can be understood from simple physical models. Polyelectrolytes with an hydrophobic backbone may provide an interesting system, that achieves a certain degree of self-organization while the relevant interactions remain relatively simple. Indeed it has been predicted in a seminal paper by Dobrynin and Rubinstein that hydrophobic polyelectrolytes should fold into an organized pearl-necklace structure where regions of high and low monomer density coexist [11]. Therefore both theoretical and experimental studies of the hydrophobic polyelectrolytes have shown a growing activity in the past few years [12, 13, 14, 15, 16, 17].

The question of the validity of the Manning condensation model for hydrophobic polyelectrolytes has been addressed experimentally by W. Essafi *et al.* [18]. The authors have measured the effective charge fraction of a highly charged hydrophobic polyelectrolyte (poly(styrene)-co-styrene sulphonate) by osmotic pressure and cryoscopy measurements. Their findings, which are recalled on Fig. (4), showed that the measured effective charge is significantly smaller than that predicted by the Manning-Oosawa theory. The aim of the present article is to provide a theoretical explanation of the counterion condensation in this system, where the presence of hydrophobic interactions influences drastically the conformation of the polymer backbone. This problem was first addressed theoretically by Dobrynin, and Rubinstein [13], who determined the phase diagram of a solution of hydrophobic polyelectrolytes as a function of solvent quality and polymer concentration. However

the question of the effective charge was not directly investigated by the authors.

## I. REVIEW OF THE PEARL-NECKLACE MODEL

Let us first recall for completeness the pearl-necklace theory of hydrophobic polyelectrolytes (for a more complete review see [14]). The polyelectrolyte solution is parameterized by its degree of polymerization  $N$ , its monomer size  $b$ , the charge fraction along the chain  $f$ , and the reduced temperature  $\tau \equiv 1 - \frac{\Theta}{T}$ , where  $\Theta$  and  $T$  denote the theta temperature of the polyelectrolyte and the temperature of the system, respectively. We note that under the conditions of bad solvent, the reduced temperature is negative  $\tau < 0$ . We let  $C$  be the average monomer concentration in the solution.

In a poor solvent, an uncharged polymer forms a globule in order to decrease its surface energy. In a similar way a drop of water adopts a spherical configuration in an hydrophobic environment. The gyration radius  $R_g$  of this polymer can be estimated by splitting the polymer into smaller units where thermal fluctuations dominate and the chain has Gaussian behavior. These units are usually called thermal blobs in the literature. It can be shown that they contain about  $\frac{1}{\tau^2}$  monomers, and have a typical size of  $b/|\tau|$ . At larger scales, the polymer tends to collapse onto itself in order to minimize its contact surface with the liquid. This can be achieved by forming a dense packing of thermal blobs. A polymer of polymerization degree  $N$  can be split into  $\tau^2 N$  subunits, under dense packing the volume occupied by the polymer is proportional to the number of subunits hence:  $R_g^3 \simeq Nb^3/|\tau|$ . The surface energy  $E_S$  associated with this configuration is given by  $k_B T$  times the number of thermal blobs in contact with the solvent. This leads to:

$$\frac{E_S}{k_B T} \simeq \frac{\tau^2 R_g^2}{b^2} \quad (1)$$

Upon charging, the electrostatic repulsion sets in, which results in a change of the globule shape. When the electrostatic repulsion energy becomes larger than the surface energy, the globule splits into several globules of smaller size consisting of  $N_g$  monomers and typical size  $R_g^3 \simeq N_g b^3/|\tau|$ . This behavior is reminiscent of the Rayleigh's instability of a charged droplet [19]. In this state, the polyelectrolyte forms a sequence of globules that are connected by strings formed of adjacent thermal blobs (see Fig. 1). In the literature, this conformation is known as the pearl-necklace. The presence of counterions will screen the electrostatic repulsion. Therefore it is important to account for their role explicitly in the balance between the surface tension and the electrostatic repulsion that governs the equilibrium structure of the necklace.

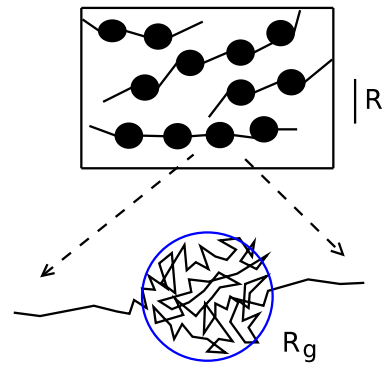


FIG. 1: (color online) Schematic drawing of the pearl-necklace structure of hydrophobic polyelectrolytes. Inside the blue (gray) circle the polymer backbone, represented by a continuous black line, is wrapped into a dense configuration of typical radius  $R_g$ , that we call pearl or globule in the text. The inset shows on a larger scale, that these pearls are connected by thin polymer strings thus forming the pearl-necklace structure. The average distance between the pearls is  $R$  (black vertical scale line).

For simplicity we assume that the main effect of the counterions is to reduce the charge of the pearls. Indeed, some counterions can be attracted inside the globules due to the attractive electrostatic forces. Therefore, the total electrostatic charge of a pearl consisting of  $N_g$  monomers is no longer given by  $qfN_g$  but by  $qf_{eff}N_g$ . Here  $q$  is the electrostatic charge of a single charged monomer and  $qf_{eff}N_g$  is the chemical charge of the pearl  $qfN_g$  minus the charge of counterions inside the pearl. The coefficient  $f_{eff}$  is called the effective charge fraction. With these definitions the electrostatic energy  $E_{el}$  of a pearl can be estimated as

$$\frac{E_{el}}{k_B T} \simeq \frac{(f_{eff}N_g)^2 \ell_B}{R_g} \simeq \frac{\tau^2 f_{eff}^2 R_g^5 \ell_B}{b^6}. \quad (2)$$

Here we have introduced  $\ell_B = q^2/(4\pi\epsilon\epsilon_0 k_B T)$  the Bjerrum length, and used the relation between the monomer number  $N_g$  and the globule radius  $R_g^3 \simeq N_g b^3/|\tau|$  ( $\epsilon$  is the solvent dielectric constant and  $\epsilon_0$  is the vacuum permittivity). We remind that for water at room temperature ( $T = 300$  K,  $\epsilon = 80$ ) the value of the Bjerrum length is  $\ell_B \approx 0.7$  nm. In its equilibrium configuration the pearl-necklace tends to balance its electrostatic and surface energies  $E_{el} \simeq E_S$ . Inserting in this equality the results of Eq. (1) and Eq. (2) leads to an expression of the globule radius  $R_g$  as a function of the effective charge fraction  $f_{eff}$ :

$$R_g^3 \simeq \frac{b^4}{\ell_B f_{eff}^2}. \quad (3)$$

## II. SCREENING OF A GLOBULE IN THE POISSON-BOLTZMANN THEORY

The problem of the effective charge of spherical globules of size  $R_g$  surrounded by their own counterions can be solved in the mean-field approximation using the Poisson-Boltzmann theory. This problem was first studied numerically and analytically by Wall and Berkowitz in [20]. It was shown that counterion condensation around such a globule is possible even in three dimension in contrast with what occurs for an impermeable globule where no counterion condensation is present for dimensions larger than two [21]. In this approach we model, a charged globule by a uniform distribution of charge density  $\rho_0 \simeq qfN_g/R_g^3 \simeq qf|\tau|/b^3$  located inside a sphere of radius  $R_g$ . The counterions are distributed inside an elementary cell of radius  $R$  at an average concentration  $n_{av} = fC$ . The size of the cell is determined by the electro-neutrality condition  $\rho_0 R_g^3 = n_{av} q R^3$ . For simplicity we assume spherical symmetry, therefore all the quantities (electrostatic potential, counterion concentration,...) depend only on the distance  $r$  to the center of the globule. Under the assumption of a Boltzmann-distribution the concentration profile  $n(r)$  of the counterions is related to the electrostatic potential  $\phi(r)$  through  $n(r) = n_{av} \exp\left(\frac{q\phi(r)}{k_B T}\right)$ . Inserting this expression into the Poisson equation  $\nabla^2 \phi = -\frac{1}{\epsilon \epsilon_0}(\rho_0(r) - qn(r))$  leads to the well-known Poisson-Boltzmann (PB) equation:

$$\nabla^2 \phi = \frac{1}{r^2} \frac{d}{dr} \left( r^2 \frac{d\phi}{dr} \right) = -\frac{\rho_0(r)}{\epsilon \epsilon_0} + \frac{n_{av} q}{\epsilon \epsilon_0} e^{\frac{q\phi}{k_B T}}, \quad (4)$$

where  $\rho_0$  is given by

$$\rho_0(r) = \begin{cases} \rho_0 \simeq q \frac{fN_g}{R_g^3} & r \leq R_g, \\ 0 & r > R_g. \end{cases} \quad (5)$$

For the spherical system with the spherical symmetry of charge distribution, at  $r = 0$  electric field is zero. Since the electrostatic field is vanish at the boundary of a neutral sphere, at  $r = R$  electric field should also be zero. Therefore the boundary conditions for the above PB equation are given as

$$\frac{d\phi(r=0)}{dr} = \frac{d\phi(r=R)}{dr} = 0. \quad (6)$$

The Debye screening length  $\lambda_D$  is given by  $\lambda_D^{-2} = 4\pi\ell_B n_{av}$ . After defining the reduced electrostatic potential,  $u \equiv q\phi/(k_B T)$ , and  $x \equiv r/\lambda_D$ , PB equation can be written as

$$\frac{d^2 u}{dx^2} + \frac{2}{x} \frac{du}{dx} = e^{u(x)} - A(x), \quad \frac{du(0)}{dx} = \frac{du(X)}{dx} = 0, \quad (7)$$

where  $A(x)$  is given by  $A(x) \equiv \rho_0(r = \lambda_D x)/(qn_{av})$  and the dimensionless versions of  $R_g$  and  $R$  are noted  $x_g$  and

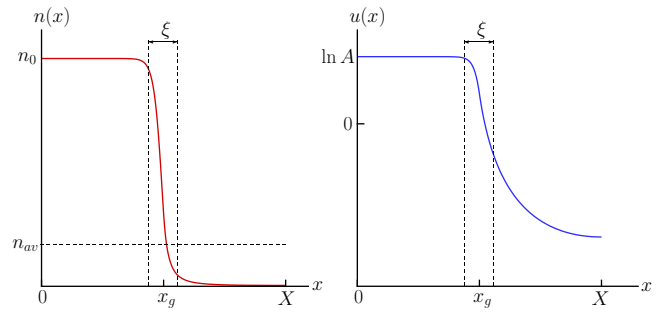


FIG. 2: Typical behavior of counterion charge distribution  $n(x)$  and effective potential  $u(x)$  in the cell. The dimensionless globule size is denoted by  $x_g$  and the cell size is denoted by  $X$ .

$X$  respectively. We will set  $A$  as the value of  $A(x)$  inside the globule:  $A(x) = A$  for  $x \leq x_g$ . With our reduced variables, the cell neutrality condition reads  $A = (X/x_g)^3$ , and  $A$  and  $x_g$  are the only free parameters of Eq. (7). We notice that  $A = \rho_0/(qn_{av}) \simeq |\tau|/(Cb^3)$  does not depend on the chemical charge  $f$ .

The fraction of counterions outside the globule  $P$  is given by the ratio  $P = \int_{x_g}^X e^u x^2 dx / \int_0^{x_g} A x^2 dx$ . With the help of Eq. (7) this expression can be reduced to a simpler form:

$$P(x_g, A) = -\frac{3}{x_g A} \frac{du(x_g)}{dx}. \quad (8)$$

If the fraction  $P$  is known, then the effective charge of the globule can be found as

$$f_{eff} = P(x_g, A)f. \quad (9)$$

It was established in [20] that the potential  $u(x)$  defined by the boundary problem Eq. (7) is a decreasing function of  $x$  and that the initial value of the potential satisfies  $e^{u(0)} \leq A$ . Physically this inequality signifies the absence of over-screening (inside the globule  $qn(r) \leq \rho_0$ ) as expected in a mean-field theory. It is possible to establish a lower bound on  $e^{u(0)}$  by rewriting Eq. (7) as an integral equation:

$$u(x) = u(0) + \int_0^x dy \left( y - \frac{y^2}{x} \right) [e^{u(y)} - A(y)]. \quad (10)$$

Since  $u(x)$  is a decreasing function, the identity Eq. (10) yields  $u(x) \leq u(0) + \frac{\min(x, x_g)^2}{6} (e^{u(0)} - A)$ . After inserting this result in the cell neutrality condition  $\int_0^X x^2 [e^{u(x)} - A(x)] dx = 0$ , one obtains:

$$1 - \frac{\log Z}{Z} \leq \frac{e^{u(0)}}{A} \leq 1, \quad \text{for } Z = \frac{x_g^2 A}{6} > e \quad (11)$$

This chain of inequalities proves that in the limit where  $x_g^2 A \gg 1$ ,  $e^{u(0)}/A \rightarrow 1$ .

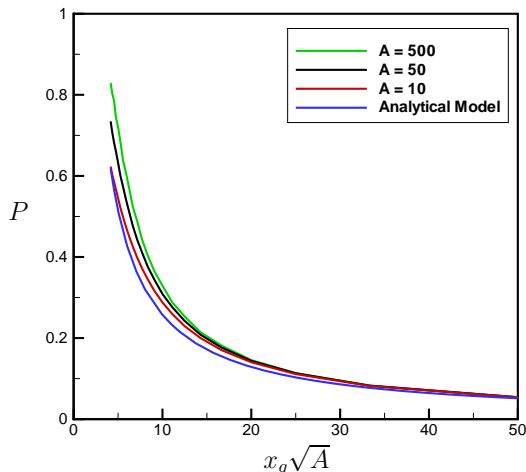


FIG. 3: Dependence of  $P$  on  $x_g\sqrt{A}$  for different values of  $A$ . From top do bottom,  $A = 500, 50, 10$  (green, black, red curves respectively). The bottom (blue) curve is the analytical prediction of Eq. (13).

The behavior of a typical solution  $u(x)$  is displayed in Fig. (2). It confirms that for large values of  $Ax_g^2$  the counterion concentration at  $x \simeq 0$ , is very close to the concentration of charged monomers inside the globule:  $e^{u(x)} \simeq A$ . As the value of  $Ax_g^2$  increases the size of the neutral region where  $u(x) \approx \ln A$  grows until it becomes of the order of globule size  $x_g$ . Therefore to keep the system electrically neutral, the counterion concentration must fall well below  $n_{av}$  at distance from the globule.

The transitions between these two regions occurs in a narrow layer of thickness  $\xi$  on the boundary of the globule, as shown in the Fig. (2). We assume that we are in the regime where  $Ax_g^2 \gg 1$ . In this regime for  $x \gtrsim x_g$ , PB equation can be estimated as

$$\frac{d^2u}{dx^2} \simeq e^u \implies \frac{\ln A}{\xi^2} \simeq A. \quad (12)$$

Therefore  $\xi$  is scaled as  $\xi \simeq 1/\sqrt{A}$ , where we have neglected the logarithmic dependence on  $A$ . Indeed in this case the contribution of  $\frac{1}{x} \frac{du}{dx}$  is of the order of  $\frac{1}{x_g} \frac{u}{\xi} \simeq \frac{\sqrt{A}}{x_g}$  and the ratio of  $\left(\frac{1}{x} \frac{du}{dx}\right) / \left(\frac{d^2u}{dx^2}\right) \simeq \frac{1}{x_g\sqrt{A}} \ll 1$ . Using Eq. (8), we can find

$$P(x_g, A) \simeq \frac{1}{x_g A} \frac{u}{\xi} \simeq \frac{6}{\sqrt{2}e} \frac{1}{x_g\sqrt{A}}, \quad (13)$$

The proportionality constant in Eq. (13) was established by ignoring the first derivative term  $\frac{1}{x} \frac{du}{dx}$  in Eq. (7). In Fig. (3), we show that there is a very good agreement between the exact and the analytical approximation results in the limit of  $Ax_g^2 \gg 1$  ( $\xi \ll x_g$ ). We also see that for a wide range of  $A$  values, our analytical theory gives a good numerical approximation for  $P$  as far as  $P \lesssim 0.4$ . For example for  $A = 500$  the relative error of

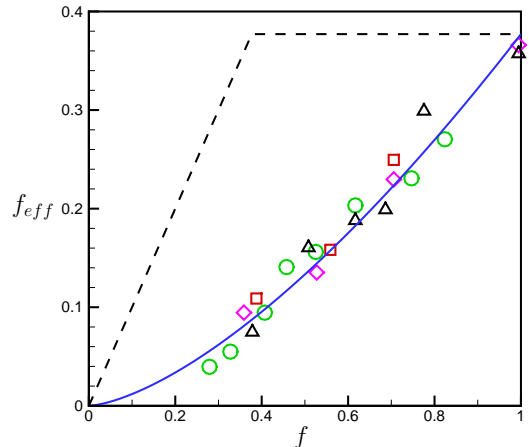


FIG. 4: Effective charge fraction  $f_{eff}$  versus the chemical charge fraction  $f$ . The experimental points were obtained in [18]. The red squares correspond to  $N = 410$ , the green circles correspond to  $N = 930$ , the purple diamonds correspond to  $N = 1320$ , and the black deltas correspond to  $N = 2400$ . The blue solid line corresponds to our theoretical model Eq. (15) with  $\sqrt{\frac{b}{|\tau|^3 \ell_B}} = 0.37$ . The dashed line corresponds to Manning's model.

our approximation is below 20% in this domain. The exact numerical results were obtained using the method described in [20].

### III. APPLICATION TO THE EFFECTIVE CHARGE OF AN HYDROPHOBIC POLYELECTROLYTE

In the regime explored experimentally by W. Essafi *et al.* [18], the value of the dimensionless parameters  $A$  can be estimated as follow. For  $|\tau| \simeq 1$ , monomer concentration  $C = 0.1 \text{ Mol L}^{-1}$  and distance between monomers  $b = 0.25 \text{ nm}$ , the expected value of  $A \simeq |\tau|/(Cb^3)$  is  $A \simeq 10^3 \gg 1$ . The value of  $x_g$  depends on both the chemical and effective charge fraction,  $f$  and  $f_{eff}$  respectively

$$x_g = \frac{R_g}{\lambda_D} \simeq \frac{|\tau|^{1/2}}{A^{1/2}} \left(\frac{\ell_B}{b}\right)^{1/6} \frac{f^{1/2}}{f_{eff}^{2/3}}. \quad (14)$$

Using Eqs. (9), (13), and (14) the effective charge can be found as

$$f_{eff} \simeq \sqrt{\frac{b}{|\tau|^3 \ell_B}} f^{3/2}. \quad (15)$$

This result predicts that the effective charge fraction  $f_{eff}$  is proportional to  $f^{3/2}$ . It is interesting to note that in this regime the effective charge does not depend on the average monomer concentration  $C$  and is an intrinsic

property of the polymer. In Fig. (4), we compare the scaling law predicted in Eq. (15) with the experimental data of Fig. (4) of ref. [18]. As one can see, there is a very good agreement between the predicted behavior and the experimental data. To summarize the experimental results are well described by the relation  $f_{eff} \simeq 0.37f^{3/2}$ . We stress that only one free proportionality constant of order one, was used to adjust the data. Thus our theory can explain, the origin of the difference between the effective charge predicted by the Manning-law recalled on Fig. (4) and that observed in experiments.

It is important to mention that in the experiments of ref. [18], only samples with relatively high chemical charge fraction  $f \geq 0.3$  were prepared, thereby limiting the range where our theory can be checked. This is related to the difficulty to stabilize solutions of hydrophobic polyelectrolytes with low chemical charge because the polyelectrolytes can form a macroscopic phase that is not soluble in the solvent. We expect that the formation of a macroscopic phase can occur if the number of monomers inside a pearl  $N_g$  becomes larger than the polymerization degree of the polymer  $N$ . In this case the polymer chains must stick together to form globules of size  $N_g \approx \frac{|\tau|b}{l_B f_{eff}^2} > N$ . Although more careful theoretical studies are needed, we think this can lead to the formation of an entangled polymer network that is not soluble anymore. We note that a detailed analysis of the possible phases and of their stability range was done in [22]. If we assume as previously, that the dimensionless factors are of order one and set  $N = 1000$  this condition for phase separation reads  $f_{eff} < 1/\sqrt{N} \simeq 0.03$  in reasonable agreement with the results displayed in Fig. (4) where no point could be obtained below this limit. We also stress that in our theory the effective charge is determined by  $N_g$  as soon as a stable pearl necklace structure forms, and is not sensitive to the polymerization degree  $N$  of the polymer. This property is very well verified in the experiment, where  $N$  was varied from  $N = 410$  to  $N = 2400$  without apparent change of the measured values of  $f_{eff}$ .

We will now comment in more details the assumptions of our model. First to establish the Eq. (15), we assumed the validity of the Eq. (13). As we have shown previously, this is justified provided  $P \ll 1$  and our numerical calculations suggest that reasonable agreement is achieved as far as  $P \lesssim 0.4$  for the experimental value of  $A \simeq 10^3$ . For the parameters used in Fig. (4), the mentioned criteria is always satisfied. Also by placing the pearls inside neutral Wigner-Seitz cells, we have ignored the effect of the interaction between neighboring pearls on the counterion distribution. However the sharp decrease of the counterion concentration on the boundary of the globule ( see Fig. (2) ) suggests that these interactions should not affect significantly the counterion distribution. We have also ignored the effect of the ions

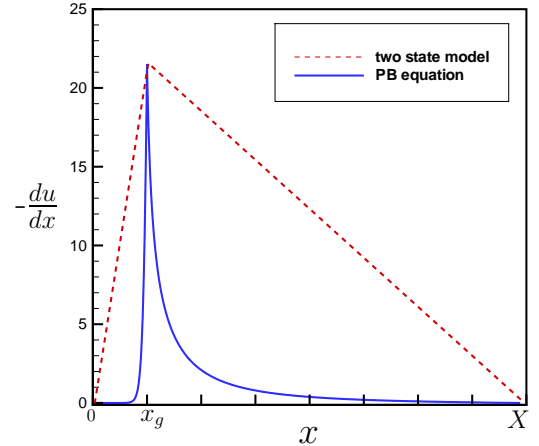


FIG. 5: Typical behavior of the dimensionless electric field  $-\frac{du}{dx}$  using either the two state model (dashed line) or our PB model (solid line). The solid line corresponds to  $x_g = 1$  and  $A = 500$ .

along the strings that connect adjacent pearls. This assumption can be checked by estimating the fraction  $s$  of the charged monomers present inside the pearls. It can be shown that

$$s \simeq \frac{1}{1 + f_{eff} \sqrt{\frac{l_B}{|\tau|^3 b}}} \simeq \frac{1}{1 + f_{eff}}, \quad (16)$$

where we have assumed that both the parameter  $\sqrt{\frac{l_B}{|\tau|^3 b}}$  and intermediate scaling constants are of order one. These assumptions are consistent with the parameters used in Fig. (4). Our theory holds as long as  $s \simeq 1$ , that is when the effective charge  $f_{eff}$  is be small. While this is clearly the case in the range of small chemical charge  $f$ , the contribution of the strings may become important when  $f \simeq 1$ . Physically we expect that around the strings, the counterions will follow the usual Manning-condensation behavior. Therefore, the effect of the strings will be mainly to keep the effective charge  $f_{eff}$  below the Manning limit  $b/l_B$ . In figure Fig. (4), the effective charge reaches this limit only at  $f \simeq 1$ ; as a result the effect of the strings is not visible and our prediction holds even up to  $f \simeq 1$ .

It is interesting to compare our findings to the results of ref. [13]. The authors considered for the first time the problem of counterion-condensation around an hydrophobic polyelectrolyte using a two-state model. They determined the fraction  $P$  by using trial counterion densities of the form  $n(r) = (1 - P)n_{av} \frac{R^3}{R_g^3}$  inside the globule (for  $r < R_g$ ), and  $n(r) = Pn_{av} \frac{R^3}{R^3 - R_g^3}$  in the outer region. This family of density is parameterized only by the parameter  $P$ . Therefore by minimizing the counterion free-energy density functional on this trial set, they could deduce an expression of  $P$  as a function of the

system parameters [23]. However for reasonable values of  $|\tau| \left(\frac{b}{\ell_B}\right)^{1/3} \simeq 1$ , and for the experimental value of  $A \simeq 10^3$ , the value of  $f_{eff}$  predicted from the equations of ref. [13] is very close to  $f$  in most of the parameter range in contradiction with the experimental results of [18]. We attribute the difference between our model and the results of [13] to the two state model used to estimate the fraction of dissociated counterions  $P$ . Indeed in the two state model the charge density is constant in the two regions inside and outside the globule. The Poisson equation then implies that in the two-state approximation, the graph of the electric field ( $-\frac{du}{dx}$  in our dimensionless units) as a function of  $x$  has a typical angle shape for all values of  $P$  as illustrated in Fig. (5). In Fig. (5) we have also compared this approximation, to the exact numerical behavior of  $-\frac{du}{dx}$ , for the typical parameters  $A = 500, x_g = 1$ . Since the charged monomers at the center of the globule are neutralized by the counterions, the true electric field distribution takes the form of a narrow peak centered at  $x_g$ . Because of its reduced family of trial functions, the two-state model can not reproduce the true behavior of the electric field. However the determination of the effective charge requires an accurate knowledge of the electric-field in the whole cell. Therefore, we believe that the two state model is not accurate enough for the determination of the effective charge. Indeed it was shown in [24] that at least a three state model is necessary in the case of a permeable droplet.

#### IV. CONCLUSIONS

In conclusion, we have developed a theory of counterion condensation around hydrophobic polyelectrolytes. Our theory is based on the pearl-necklace model for the polyelectrolyte backbone. We assumed that the pearls are permeable to the counterions, and use analytic results on the Poisson-Boltzmann equation to establish the fraction of counterions condensed inside the pearls. This allows us to establish a power law dependence of the effective charge  $f_{eff}$  on the chemical charge  $f$ :  $f_{eff} \propto f^{3/2}$ . This prediction is in very good agreement with recent experimental results by W. Essafi *et al.* [18] and explains the large deviation from the Manning law observed in these experiments. While our main results concern the effective charge of hydrophobic polyelectrolytes, the scaling laws that we derived may also apply to other areas of physics and chemistry where the Poisson-Boltzmann equation plays an important role.

#### ACKNOWLEDGMENTS

We thank D. Baigl, M. Rubinstein and E. Trizac for fruitful discussions and precious remarks. One of us, A.

Chepelianskii, acknowledges the support of Ecole Normale Supérieure de Paris.

- 
- [1] G. S. Manning, J. Chem. Phys. **51**, 924 (1969).
  - [2] F. Oosawa, *Polyelectrolytes* (Marcel Dekker, New York, 1971).
  - [3] Y. Kantor, H. Li, and M. Kardar Phys. Rev. Lett. **69**, 61 (1992).
  - [4] J.-L. Barrat and J.-F. Joanny, Advances in Chemical Physics (S. Rice, I. Prigogine eds; J. Wiley) **54**, 1 (1996)
  - [5] C. Holm, J.F. Joanny, K. Kremer, R.R Netz, P. Reineker, C.Seidel, T.A. Vigis, R.G Winkler, Adv. Polym. Sci **166** 67 (2004)
  - [6] V.A. Bloomfield, D.M. Crothers and I. Tinoco, *Nucleic Acids Structures, Properties and Functions* (University Science Books, Sausalito, CA, 2000).
  - [7] J. R. Philif and R. A. Wooding, J. Chem. Phys. **52**, 953 (1970).
  - [8] B. O'Shaughnessy and Q. Yang, Phys. Rev. Lett. **94**, 048302 (2005).
  - [9] P. Gonzalez-Mozuelos and M. Olvera de la Cruz, J. Chem. Phys **103** 22 (1995)
  - [10] B. Alberts, D. Bray, A. Johnson, J. Lewis, M. Raff, K. Roberts, and P. Walter, *Essential Cell Biology* (Garland Publishing, New York, 1998).
  - [11] A. V. Dobrynin, M. Rubinstein, and S. P. Obukhov, Macromolecules **29**, 2974 (1996).
  - [12] E. Raphael and J.-F. Joanny Europhys. Lett., **13** (7), 623 (1990)
  - [13] A. V. Dobrynin and M. Rubinstein, Macromolecules **34**, 1964 (2001).
  - [14] A. V. Dobrynin and M. Rubinstein, Prog. Polym. Sci. **30**, 1049 (2005).
  - [15] M. D. Carbajal-Tinoco and C. E. Williams, Europhys. Lett., **52**, 284 (2000).
  - [16] M.-J. Lee, M. M. Green, F. Mikes, and H. Morawetz, Macromolecules, **35**, 4216 (2002).
  - [17] A. Kyriy, G. Gorodyska, S. Minko, W. Jaeger, P. Stepanek, and M. Stamm, J. Am. Chem. Soc. **124**, 13454 (2002).
  - [18] W. Essafi, F. Lafuma, D. Baigl, and C. E. Williams, Europhys. Lett. **71**, 938 (2005).
  - [19] L. Rayleigh, Philos. Mag. **14**, 184 (1882).
  - [20] F.T. Wall and J. Berkowitz, J. Chem. Phys. **26**, 114 (1957).
  - [21] B.H. Zimm and M. Le Bret J. Biomolecular Structure and Dynamics, **1**, 461 (1983)
  - [22] H. Schiessel, and P. Pincus, Macromolecules **31**, 7953 (1998)
  - [23] The final result is given in Eq. (21) of ref. [13] where  $P = x$ .
  - [24] M. Deserno, Eur. Phys. J. E, **6**, 163 (2001)